

Extended Phase Space Thermodynamics for Dyonic Black Holes with a Power Maxwell Field

Feiyu Yao^{a*} and Jun Tao^{a†}

^a*Center for Theoretical Physics, College of Physics,
Sichuan University, Chengdu, 610064, China*

Abstract

In this paper, we investigate the thermodynamics of dyonic black holes with the presence of power Maxwell electromagnetic field in the extended phase space, which includes the cosmological constant Λ as a thermodynamic variable. For a generic power Maxwell black hole with the electric charge and magnetic charge, the equation of state is given as the function of rescaled temperature \tilde{T} in terms of other rescaled variables \tilde{r}_+ , \tilde{q} and \tilde{h} , where r_+ is the horizon radius, q is the electric charge and h is some magnetic parameter. For some values of \tilde{q} and \tilde{h} , the phase structure of the black hole is uniquely determined. Moreover the peculiarity of multiple temperature with some fixed parameter configurations results in more rich phase structures. Focusing on the power Maxwell Lagrangian with $\mathcal{L}(s) = s^2$, we obtain the corresponding phase diagrams in the \tilde{q} - \tilde{h} plane, then analyse the black holes phase structure and critical behaviour. For this case, the critical line is semi-infinite and extends to $\tilde{h} = \infty$. We also examine thermal stabilities of these black holes.

*Electronic address: yaofeiyu@stu.scu.edu.cn

†Electronic address: taojun@scu.edu.cn

Contents

I. Introduction	2
II. Dyonic PM AdS Black Hole	4
III. 8-d Dyonic PM AdS Black Hole with $p=2$	10
IV. Discussion and Conclusion	18
V. Acknowledgement	20
References	20

I. INTRODUCTION

Black holes are intriguing concepts from the two cornerstones of modern theoretical physics: General Relativity and Quantum Field Theory. Classically black holes absorbed all matter and emitted nothing. Superficially they had neither temperature nor entropy, and were characterized by only a few basic parameters: mass, angular momentum, and charge (if any) [1]. However all of this were changed by the advent of quantum field theory in curved spacetime. The first indication linking black holes and thermodynamics came from Hawking's area theorem [2], which states that the area of the event horizon of a black hole can never decrease. Bekenstein subsequently noticed the resemblance between this area law and the second law of thermodynamics [3], proposing that each black hole should be assigned an entropy proportional to the area of its event horizon [4]. Analogous to the laws of thermodynamics, Bardeen, Carter and Hawking soon established the four laws of black hole mechanics [5], where the surface gravity corresponds to the temperature. Since Hawking discovered that black holes do emit radiation with a blackbody spectrum [6], the idea of black hole thermodynamics has convinced most physicists. And over the past four decades, a preponderance of evidence suggested that it is a meaningful subject.

According to the sign of cosmological constant Λ , black holes can be classified into asymptotically de Sitter (dS) black holes ($\Lambda > 0$), asymptotically Anti-de Sitter (AdS) black holes ($\Lambda < 0$) and asymptotically flat black holes ($\Lambda=0$). Sufficiently large asymptotically AdS

(as compared to the AdS radius l) black holes, unlike asymptotically flat black holes, have positive specific heat and can be in stable equilibrium at a fixed temperature [7]. Moreover asymptotically AdS black holes, unlike asymptotically dS BH [8], only have one horizon and one can define a good notion of the asymptotic mass. So the asymptotically AdS black holes are always popular subjects. Studying the phase transitions of asymptotically AdS black holes is primarily motivated by AdS/CFT correspondence [9]. Hawking and Page showed that a first-order phase transition occurs between Schwarzschild AdS black holes and thermal AdS space [7], which was later understood as a confinement/deconfinement phase transition in the context of the AdS/CFT correspondence [10]. For Reissner-Nordstrom (RN) AdS black holes, authors of [11, 12] showed that their critical behavior is similar to that of a Van der Waals liquid gas phase transition.

Later, the asymptotically AdS black holes were studied in the context of extended phase space thermodynamics, where the cosmological constant is interpreted as thermodynamic pressure [13, 14]. In this case, the black hole mass should be understood as enthalpy instead of the internal energy; the first law was modified [15]. The P - V criticality study has been explored for various AdS black holes [16–21]. It showed that the P - V critical behaviors of AdS black holes are similar to that of a Van der Waals liquid gas system.

Nonlinear electrodynamics (NLED) is an effective model incorporating quantum corrections to Maxwell electromagnetic theory. Coupling NLED to gravity, various NLED charged black holes were derived and discussed in a number of papers [22–31]. The thermodynamics of generic NLED black holes in the extended phase space have been considered in [32–36]. And various particular NLED black holes were also considered, e.g., Born-Infeld AdS black holes [37, 38], power Maxwell invariant black holes [39–41], nonlinear magnetic-charged dS black holes [42].

Among the various NLED, straightforward generalization of Maxwell’s theory leads to the so called power Maxwell (PM) theory described by a Lagrangian density of the form $\mathcal{L}(s) = s^p$, where s is the Maxwell invariant, and p is an arbitrary rational number. Clearly the special value $p = 1$ corresponds to linear electrodynamics. The solutions of PM charged black holes and their interesting thermodynamics and geometric properties have been examined in [26, 43–50].

The PM theory is a toy model to generalize Maxwell theory which reduces to it for $p = 1$. One of the most important properties of the PM model in d -dimensions occurs

when $p = d/4$, where the PM theory becomes conformally invariant and the trace of energy-momentum tensor vanishes, such as Maxwell theory in four-dimensions. On the other hand, taking into account the applications of the AdS/CFT correspondence to superconductivity, it has been shown that the PM theory makes crucial effects on the condensation as well as the critical temperature of the superconductor and its energy gap [51].

A substantial gap in these studies is the absence of dyonic solution. Authors of [52] derived a scheme of finding dyonic solution in NLED coupled to GR by quadratures for an arbitrary Lagrangian function $L(s)$ and a dyonic solution for the truncated Born-Infeld theory. However there are still not many papers devoted to studies of specific cases with dyonic solution.

In this paper, We first investigate the thermodynamic behavior of generic d -dimensional dyonic PM black holes in the extended phase space. Then, we turn to study the phase structure and critical behavior of 8-dimensional dyonic PM black holes with an power exponent of 2 by studying the phase diagrams in the $q/l^{4.5}$ - $h/l^{1.5}$ plane. After this Introduction, we derive d -dimensional dyonic PM black hole solutions and discuss thermodynamic properties of the black hole in section II. In section III, we study the phase structure and critical behavior of 8-dimensional dyonic PM AdS black holes with an power exponent of 2. The phase diagram for the black hole in the $q/l^{4.5}$ - $h/l^{1.5}$ plane is given in FIG. 5, from which one can read the black hole's phase structure and critical behavior. We also explore thermal stabilities of these black holes. We summarize our results in section IV. We will use the units $\hbar = c = 16\pi G = 1$ for simplicity.

II. DYONIC PM ADS BLACK HOLE

In this section, we derive the d -dimensional dyonic PM asymptotically AdS black hole solution in the Einstein gravity and verify the thermodynamic properties of the black hole. We first consider a d -dimensional model of gravity coupled to a PM nonlinear electromagnetic field with action given by

$$S_{\text{Bulk}} = \int d^d x \sqrt{-g} [R - 2\Lambda + \mathcal{L}(s)], \quad (1)$$

where

$$\Lambda = -\frac{(d-1)(d-2)}{2l^2} \quad (2)$$

is cosmological constant,

$$s = \frac{1}{4} F_{\mu\nu} F^{\mu\nu} \quad (3)$$

is the maxwell invariant, $F = dA = \partial_\mu A_\nu - \partial_\nu A_\mu$ and A_μ is the gauge potential. In our case the Lagrangian density has the following form

$$\mathcal{L}(s) = s^p. \quad (4)$$

Taking the variation of the action (1) with respect to $g_{\mu\nu}$ and A_μ , one can get the equations of motion, they are

$$R_{\mu\nu} - \frac{1}{2} R g_{\mu\nu} - \frac{(d-2)(d-1)}{2l^2} g_{\mu\nu} = \frac{T_{\mu\nu}}{2}, \quad (5)$$

$$\partial_\mu (\sqrt{-g} G^{\mu\nu}) = 0, \quad (6)$$

where

$$T_{\mu\nu} = g_{\mu\nu} \mathcal{L}(s) + \frac{\partial \mathcal{L}(s)}{\partial s} F_\mu{}^\rho F_{\nu\rho} \quad (7)$$

is energy-momentum tensor and we defined the auxiliary field

$$G^{\mu\nu} = \frac{\partial \mathcal{L}(s)}{\partial s} F^{\mu\nu}. \quad (8)$$

To construct a dyonic black hole solution in asymptotically AdS spacetime, we take the following ansatz for the metric and the gauge potential

$$ds^2 = -f(r) dt^2 + \frac{1}{f(r)} dr^2 + r^2 d\Omega_{d-2}^2, \quad (9)$$

$$A = A_t(r) dt - h \left(\prod_{i=1}^{d-4} \sin^2 \theta_i \right) \cos \theta_{d-3} d\theta_{d-2}, \quad (10)$$

where $d\Omega_{d-2}^2$ is the metric of $(d-2)$ -sphere (only consider the case of positive constant curvature, i.e. $k=1$),

$$d\Omega_1^2 = d\theta_1^2, \quad (11)$$

$$d\Omega_{n+1}^2 = d\Omega_n^2 + \left(\prod_{i=1}^n \sin^2 \theta_i \right) d\theta_{n+1}^2. \quad (12)$$

Then the equations of motion read

$$\frac{(d-2)}{2} r f(r)' + \frac{(d-2)(d-3)}{2} [f(r) - 1] - \frac{(d-2)(d-1)r^2}{2l^2} = \frac{r^2}{2} [\mathcal{L}(s) + G^{rt} A_t'(r)], \quad (13)$$

$$\partial_r (r^{d-2} G^{rt}) = 0, \quad (14)$$

$$\partial_{\theta_{d-3}} (\sin \theta_{d-3} G^{\theta_{d-3} \theta_{d-2}}) = 0, \quad (15)$$

and plugging eqn. (10) into eqn. (3) and eqn. (8) results in

$$s = \frac{A_t^2(r)}{2} - \frac{h^2}{2r^4} \text{ and } G^{rt} = -\frac{\partial \mathcal{L}(s)}{\partial s} A_t'(r). \quad (16)$$

Eqn. (15) can result in $\partial_{\theta_{d-3}} h = 0$ and the rest equations of motion can be derived from eqn. (13) and eqn. (14). Now $A_t'(r)$ can be determined by eqn. (14), which leads to

$$\frac{\partial \mathcal{L}(s)}{\partial s} A_t'(r) = \frac{q}{r^{d-2}}, \quad (17)$$

where q is a constant. Moreover integrating eqn. (13), we have

$$f(r) = 1 + \frac{r^2}{l^2} - \frac{m}{r^{d-3}} - \frac{1}{(d-2)r^{d-3}} \int_r^\infty dr r^{d-2} \left[\mathcal{L} \left(\frac{A_t^2(r)}{2} - \frac{h^2}{2r^4} \right) - \frac{q}{r^{d-2}} A_t'(r) \right], \quad (18)$$

where m is a constant. At the horizon $r = r_+$, the Hawking temperature of the black hole is given by

$$T = \frac{f'(r_+)}{4\pi}, \quad (19)$$

so one can have

$$T = \frac{1}{4\pi r_+} \left\{ d - 3 + \frac{(d-1)r_+^2}{l^2} + \frac{1}{d-2} r_+^2 \left[\mathcal{L} \left(\frac{A_t^2(r)}{2} - \frac{h^2}{2r^4} \right) - \frac{q}{r^{d-2}} A_t'(r_+) \right] \right\}, \quad (20)$$

which results from plugging $f(r_+) = 0$ into eqn. (13).

Then the electric charge is [53]

$$Q = \int_S \bar{F} = \int \left(\prod_1^{d-2} d\theta_i \right) \bar{F} = \int \left(\prod_{i=1}^{d-2} d\theta_i \right) \sqrt{-g} \frac{q}{r^{d-2}} = \omega_{d-2} q, \quad (21)$$

where

$$\bar{F} = \frac{\partial \mathcal{L}}{\partial s} (*F), \quad (22)$$

with ω_{d-2} being the volume of the unit $(d-2)$ -sphere:

$$\omega_{d-2} = \frac{2\pi^{\frac{d-1}{2}}}{\Gamma\left(\frac{d-1}{2}\right)}. \quad (23)$$

Moreover, the mass can be extracted by comparison to a reference background, e.g., vacuum AdS. So the mass can be determined by the Komar integral

$$M = \frac{d-2}{8\pi(d-3)} \int_{\partial\Sigma} dx^{d-2} \sqrt{\gamma'} (\sigma_\mu n_\nu \nabla^\mu K^\nu) - M_{\text{AdS}}, \quad (24)$$

where K^μ is the Killing vector associated with t , and M_{AdS} is Komar integral associated with K^μ for vacuum AdS space

$$M_{\text{AdS}} = \frac{d-2}{8\pi(d-3)} \int_{\partial\Sigma} dx^{d-2} \sqrt{\gamma'} \left(\frac{r}{l^2} \right), \quad (25)$$

and γ' is the induced metric of $\partial\Sigma$, which is the boundary of Σ . σ_μ is the unit normal vector of Σ and n_μ is the unit outward-pointing normal vector. Setting Σ and $\partial\Sigma$ are a constant- t hypersurface and a $(d-2)$ -sphere at $r = \infty$.

Using

$$\sigma_\mu = (-f^{\frac{1}{2}}, 0, 0, 0, \dots), \quad (26)$$

$$n_\mu = (0, f^{-\frac{1}{2}}, 0, 0, \dots), \quad (27)$$

one can have

$$\sigma_\mu n_\nu \nabla^\mu K^\nu = \frac{1}{2} f'(r). \quad (28)$$

It is shown that in some case, which is

$$d-1 < 4p < 2d-2, \quad (29)$$

one can have

$$\frac{1}{2} f'(r) = \frac{r}{l^2} + \frac{(d-3)m}{2r^{d-2}} + O(r^{2-d}) \quad (30)$$

at spatial infinity, whether it hold or not is determined by the relationship of power exponent p and dimension d . When it hold, we have

$$M = \frac{d-2}{16\pi} \omega_{d-2} m. \quad (31)$$

In the following, we study the thermodynamics of the dyonic PM AdS black hole solution in the extended phase space, where the cosmological constant is interpreted as thermodynamic pressure and treated as a thermodynamic variable in its own right. The mass of the black hole is no longer regarded as internal energy, it is identified with the chemical enthalpy.

In terms of the horizon radius r_+ , the mass can be rewritten as

$$M = \frac{d-2}{16\pi} \omega_{d-2} \left\{ r_+^{d-3} + \frac{r_+^{d-1}}{l^2} - \frac{1}{d-2} \int_{r_+}^{\infty} dr r^{d-2} \left[\mathcal{L} \left(\frac{A_t'^2(r)}{2} - \frac{h^2}{2r^4} \right) - A_t'(r) \frac{q}{r^{d-2}} \right] \right\} \quad (32)$$

where we have used eqn. (31).

Adding that the Gibbs free energy F can be expressed by the Euclidean action S^E [32]:

$$F = M - TS, \quad (33)$$

where the entropy of the black hole is one-quarter of the horizon area

$$S = \frac{r_+^{d-2} \omega_{d-2}}{4}. \quad (34)$$

We have expressed thermodynamics quantities (F , M and S) as the functions of the horizon radius r_+ , q (proportional to the electric charge Q), h (associated with magnetic charge) and the AdS radius l (the pressure $P = (d-1)(d-2)/l^2$). Now we need to express the thermodynamics quantities in terms of T , q , h and P by solving the equation of state for

$$r_+ = r_+(T, q, l, h). \quad (35)$$

So we first rescale the T , which becomes

$$\tilde{T} = \frac{1}{4\pi\tilde{r}_+} \left\{ d - 3 + (d-1)\tilde{r}_+^2 + \frac{\tilde{r}_+^2}{d-2} \left[\left(\frac{\tilde{A}'_t{}^2(r_+)}{2} - \frac{\tilde{h}^2}{2\tilde{r}_+^4} \right)^p - \tilde{A}'_t(r_+) \frac{\tilde{q}}{\tilde{r}_+^{d-2}} \right] \right\}, \quad (36)$$

where

$$\tilde{r}_+ = r_+ l^{-1}, \quad \tilde{q} = q l^{-\frac{1}{p}-d+4}, \quad \tilde{A}'_t(r_+) = l^{\frac{1}{p}} A'_t(r_+), \quad \tilde{h} = h l^{\frac{1}{p}-2}, \quad \tilde{T} = Tl, \quad (37)$$

and p is the power of

$$\mathcal{L}(s) = s^p. \quad (38)$$

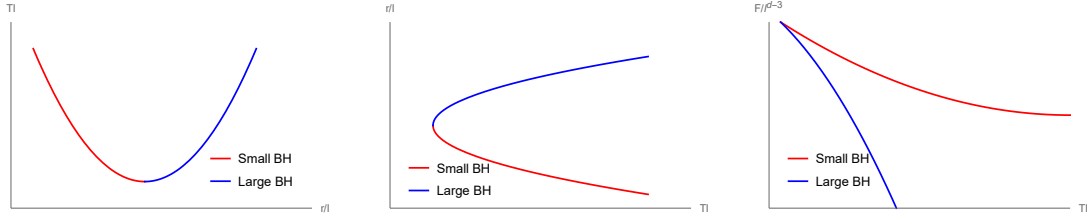
Then $\tilde{A}'_t(r_+)$ is determined by

$$\left(p \frac{\tilde{A}'_t{}^2(r_+)}{2} - \frac{\tilde{h}^2}{2\tilde{r}_+^4} \right)^{p-1} \tilde{A}'_t(r_+) = \frac{\tilde{q}}{\tilde{r}_+^{d-2}}, \quad (39)$$

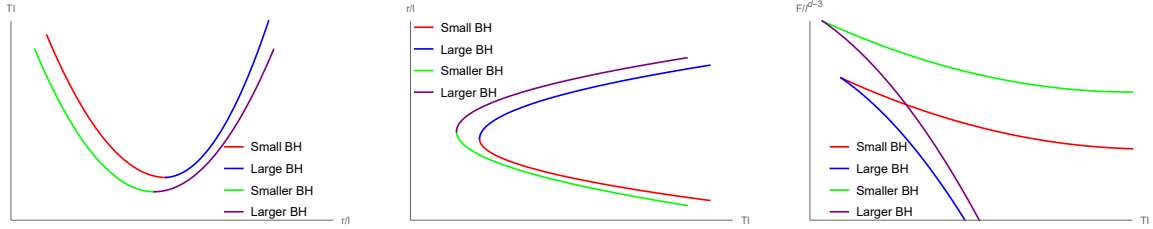
which usually cannot be solved analytically and has multiple solutions when p is large. After that, solving eqn. (36), \tilde{r}_+ can be expressed as a function of \tilde{T} , \tilde{q} and \tilde{h} : $\tilde{r}_+ = \tilde{r}_+(\tilde{T}, \tilde{q}, \tilde{h})$. With $\tilde{r}_+ = \tilde{r}_+(\tilde{T}, \tilde{q}, \tilde{h})$, one can express the thermodynamic quantities in terms of \tilde{T} , \tilde{q} and \tilde{h} , e.g., the Gibbs free energy is given by

$$\tilde{F} \equiv F/l^{d-3} = \tilde{F}(\tilde{T}, \tilde{q}, \tilde{h}). \quad (40)$$

The rich phase structure of the black hole comes from solving eqn. (36), i.e., $\tilde{T} = \tilde{T}(\tilde{r}_+, \tilde{q}, \tilde{h})$, for \tilde{r}_+ . If $\tilde{T}(\tilde{r}_+, \tilde{q}, \tilde{h})$ is a monotonic function with respect to \tilde{r}_+ for some values



(a) Branches around a local minimum of $\tilde{T} = \tilde{T}_{\min}$.



(b) Branches around a local maximum of $\tilde{T} = \tilde{T}_{\max}$ when $\tilde{T} = \tilde{T}(\tilde{r}_+; \tilde{q}, \tilde{h})$ is multivalued.

FIG. 1: Branches of black holes around local extremums of $\tilde{T} = \tilde{T}_{\min}$. Right panels: Gibbs free energy vs temperature. The blue branches are thermodynamically preferred and thermally stable. The red ones are thermally unstable. Below column: the case of more than one $\tilde{T}(\tilde{r}_+, \tilde{q}, \tilde{h})$ with some fixed \tilde{q} and \tilde{h} .

of \tilde{q} and \tilde{h} , there would be only one branch for the black hole. More often, with fixed \tilde{q} and \tilde{h} , there exists a local minimum/maximum for $\tilde{T}(\tilde{r}_+, \tilde{q}, \tilde{h})$ at $\tilde{r}_+ = \tilde{r}_{+, \min}/\tilde{r}_+ = \tilde{r}_{+, \max}$. In this case, there are more than one branch for the black hole. In FIG. 1(a), we plot two branches, namely small BH and large BH, around a local minimum of $\tilde{T} = \tilde{T}_{\min}$. The Gibbs free energy of these two branches is displayed in the right panel of FIG. 1(a). Since $\partial\tilde{F}(\tilde{T}, \tilde{q}, \tilde{h})/\partial\tilde{T} = -4\pi^6\tilde{r}_+^6$, the upper branch is small BH while the lower one is large BH, which means that the large BH branch is thermodynamically preferred. Similarly, there are also two branches around a local maximum of \tilde{T} . In this case the upper/lower branch is large/small BH since it has more/less negative slope and the small BH branch is thermodynamically preferred in this case. In general, one might need to figure out how the existence of local extremums depends on values of \tilde{Q} and \tilde{h} to study the phase structure of the black hole.

Moreover, since there are more than one solution by solving the eqn. (39) for some values of \tilde{q} and \tilde{h} , there are more than one $\tilde{T}(\tilde{r}_+, \tilde{q}, \tilde{h})$ with some fixed \tilde{q} and \tilde{h} , which means more one set of $\tilde{r}_{+i} = \tilde{r}_{+i}(\tilde{T}, \tilde{q}, \tilde{h})$. And every set of $\tilde{r}_{+i}(\tilde{T}, \tilde{q}, \tilde{h})$ maybe still have many branches. In FIG. 1(b), we show a possible simple case, every panel is corresponding to those of FIG.

1(a). And of course it could be more complicated.

After the black hole's branches are obtained, it is easy to check their thermodynamic stabilities against thermal fluctuations. The thermal stability of the branch follows from the specific heat $C > 0$. The specific heat we need is

$$C_{Q,h,P} = T \left(\frac{\partial S}{\partial T} \right)_{Q,h,P} = l^{d-2} (d-2) \tilde{T} \frac{\tilde{r}_+^{d-3} \omega_{d-2}}{4} \left(\frac{\partial \tilde{r}_+}{\partial \tilde{T}} \right), \quad (41)$$

since ω_{d-2} is also positive, the sign of $\tilde{T}'(\tilde{r}_+)$ determines the thermodynamic stabilities.

III. 8-D DYONIC PM ADS BLACK HOLE WITH P=2

In this section, we focus on a specific example. For simplicity, we consider the case that the power exponent is 2, and we consider $8-d$ spacetime in order to satisfying the condition of eqn. (29).

When $d = 8$, $p = 2$ the mass becomes

$$M = \frac{2}{5} \pi^2 \left\{ r_+^5 + \frac{r_+^7}{l^2} - \frac{1}{6} \int_{r_+}^{\infty} dr r^6 \left[\mathcal{L} \left(\frac{A_t'^2(r)}{2} - \frac{h^2}{2r^4} \right) - A_t'(r) \frac{q}{r^6} \right] \right\} \quad (42)$$

and the electric charge

$$Q = \frac{16\pi^3}{15} q, \quad (43)$$

where we have used eqn. (32) and eqn. (21). And the eqn. (36) and eqn. (34) become

$$\tilde{T} = \frac{1}{4\pi\tilde{r}_+} \left\{ 5 + 7\tilde{r}_+^2 + \frac{\tilde{r}_+^2}{6} \left[\mathcal{L} \left(\frac{\tilde{A}_t'^2(r_+)}{2} - \frac{\tilde{h}^2}{2\tilde{r}_+^4} \right) - \tilde{A}_t'(r_+) \frac{\tilde{q}}{\tilde{r}_+^6} \right] \right\}, \quad (44)$$

$$S = \frac{4}{15} \pi^3 r_+^6, \quad (45)$$

where

$$\tilde{r}_+ = r_+ l^{-1}, \quad \tilde{q} = q l^{-4.5}, \quad \tilde{A}_t'(r_+) = l^{0.5} A_t'(r_+), \quad \tilde{h} = h l^{-1.5}, \quad \tilde{T} = T l. \quad (46)$$

Moreover, the Gibbs free energy is given by

$$F = M - T S \quad (47)$$

and

$$\tilde{F} \equiv F/l^5 = \tilde{F}(\tilde{T}, \tilde{q}, \tilde{h}). \quad (48)$$

The case of $p = 2$ is described by the Lagrangian density

$$\mathcal{L}(s) = s^2, \quad (49)$$

and solving eqn. (39) for $\tilde{A}'_t(r)$ gives

$$\tilde{A}'_{ti}(r_+) = \frac{2\tilde{h}}{\sqrt{3\tilde{r}_+^2}} \cos \left[\frac{1}{3} \arccos \left(\frac{3\sqrt{3}\tilde{q}}{2\tilde{h}^3} \right) - \frac{2\pi}{3}(i-1) \right], \quad i = 1, 2, 3, \quad (50)$$

where $\tilde{A}'_{t2}(r_+)$ and $\tilde{A}'_{t3}(r_+)$ exist only if $3\sqrt{3}\tilde{q}/2\tilde{h}^3 \leq 1$ for $\tilde{h}\tilde{q} > 0$; $\tilde{A}'_{t2}(r_+)$ and $\tilde{A}'_{t1}(r_+)$ exist only if $3\sqrt{3}\tilde{q}/2\tilde{h}^3 \geq -1$ for $\tilde{h}\tilde{q} < 0$.

The equations of state (36) become

$$\tilde{T}_i = \frac{1}{4\pi\tilde{r}_+} \left\{ 5 + 7\tilde{r}_+^2 + \frac{\tilde{r}_+^2}{6} \left[\left(\frac{\tilde{A}'_{ti}(r_+)}{2} - \frac{\tilde{h}^2}{2\tilde{r}_+^4} \right)^2 - A'_{ti}(r_+) \frac{\tilde{q}}{\tilde{r}_+^6} \right] \right\} \quad (51)$$

$$= \frac{1}{4\pi\tilde{r}_+} \left\{ 5 + 7\tilde{r}_+^2 + \frac{\tilde{r}_+^2}{6} \left[\left(\frac{2\tilde{h}^2}{3\tilde{r}_+^4} C_i^2(\tilde{h}, \tilde{q}) - \frac{\tilde{h}^2}{2\tilde{r}_+^4} \right)^2 - \frac{2\tilde{h}\tilde{q}}{\sqrt{3}\tilde{r}_+^8} C_i(\tilde{h}, \tilde{q}) \right] \right\} \quad (52)$$

$$= \frac{1}{4\pi\tilde{r}_+} \left[5 + 7\tilde{r}_+^2 + \frac{\tilde{h}^4}{6\tilde{r}_+^6} D_i(\tilde{h}, \tilde{q}) \right], \quad (53)$$

and we have defined two functions that are independent of \tilde{r}_+ for later use

$$C_i(\tilde{h}, \tilde{q}) = \cos \left[\frac{1}{3} \arccos \left(\frac{3\sqrt{3}\tilde{q}}{2\tilde{h}^3} \right) - \frac{2\pi}{3}(i-1) \right] \quad (i = 1, 2, 3), \quad (54)$$

$$D_i(\tilde{h}, \tilde{q}) = \left[\left(\frac{4C_i^2(\tilde{h}, \tilde{q})}{3} - 1 \right) \frac{1}{2} \right]^2 - C_i(\tilde{h}, \tilde{q}) \frac{2\tilde{q}}{\sqrt{3}\tilde{h}^3}. \quad (55)$$

Setting $3\sqrt{3}\tilde{q}/2\tilde{h}^3 \equiv x$, we have

$$C_i(x) \equiv \cos \left[\frac{1}{3} \arccos x - \frac{2\pi}{3}(i-1) \right] \quad (i = 1, 2, 3), \quad (56)$$

$$D_i(x) \equiv \left\{ \left[\left(\frac{4C_i^2(x)}{3} - 1 \right) \frac{1}{2} \right]^2 - xC_i(x) \frac{4}{9} \right\}, \quad (57)$$

and we can see that $\tilde{h}^4 D_i(x)$ completely determines the dependence of $\tilde{T}_i(\tilde{r}_+)$ on \tilde{r}_+ ,

$$\tilde{T}_i(\tilde{r}_+, \tilde{h}, x) = \frac{1}{4\pi\tilde{r}_+} \left[5 + 7\tilde{r}_+^2 + \frac{\tilde{h}^4}{6\tilde{r}_+^6} D_i(x) \right], \quad (58)$$

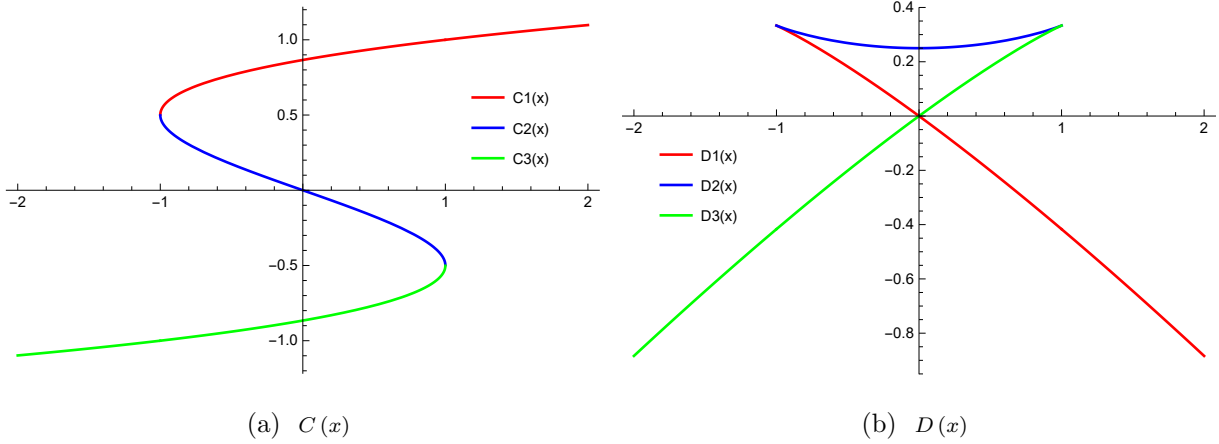


FIG. 2: $C(x)$ and $D(x)$, where $x \equiv \frac{3\sqrt{3}\tilde{q}}{2\tilde{h}^3}$.

which also tells us that three curves of $\tilde{T}_i(\tilde{r}_+; \tilde{h}, x)$ are never intersect with fixed \tilde{h}, x . Moreover, we can write the rescaled Gibbs free energy as

$$\tilde{F} = \frac{12\pi^2\tilde{r}_+^5}{5} + \frac{16\pi^2\tilde{r}_+^7}{5} - \frac{28}{15}\pi^3\tilde{r}_+^6\tilde{T}, \quad (59)$$

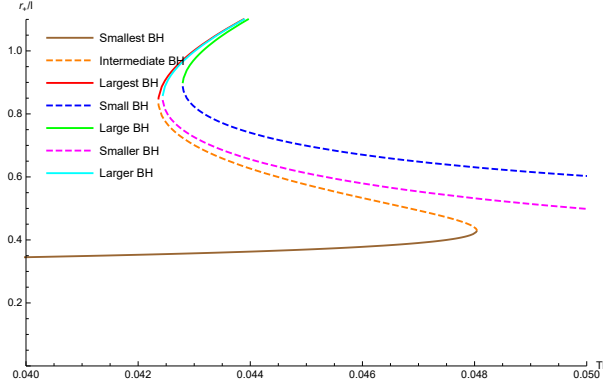
and it is also easy to see that three curves of $F(\tilde{T}_i; \tilde{h}, x)$ are never intersect with fixed \tilde{h}, x .

To study the behavior of local extremums of $\tilde{T}_i(\tilde{r}_+)$, we consider the equation $\tilde{T}_i''(\tilde{r}_+) = 0$, which becomes

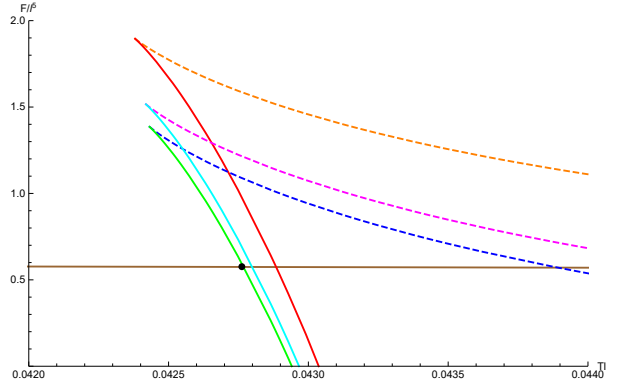
$$\frac{d^2\tilde{T}_i}{d\tilde{r}_+^2} = \frac{10}{4\pi\tilde{r}_+^3} + \frac{7\tilde{h}^4}{3\pi\tilde{r}_+^9}D_i(\tilde{h}, \tilde{q}) = 0. \quad (60)$$

For $\tilde{h}\tilde{q} > 0$, since $D_2(\tilde{h}, \tilde{q}) > 0$ and $D_3(\tilde{h}, \tilde{q}) > 0$, which is shown in FIG. 2(b), only $\tilde{T}_1''(\tilde{r}_+) = 0$ has a root and only has one root. And when $\tilde{h}\tilde{q} < 0$, only $\tilde{T}_3''(\tilde{r}_+) = 0$ has and only has a root. From FIG. 2(b), we can find $D_1(x)$ is symmetry with $D_3(x)$, which means $\tilde{T}_1(\tilde{r}_+)/\tilde{T}_3(\tilde{r}_+)$ for $\tilde{h}\tilde{q} > 0$ is identical to $\tilde{T}_3(\tilde{r}_+)/\tilde{T}_1(\tilde{r}_+)$ for $\tilde{h}\tilde{q} < 0$. So we only discuss the case of $\tilde{q} > 0, \tilde{h} > 0$ in the following. With solutions of $\tilde{T}_i''(\tilde{r}_+) = 0$, it is easy to analyze the existence of the local extremums of $\tilde{T}'(\tilde{r}_+)$, results of which are summarized in Table I.

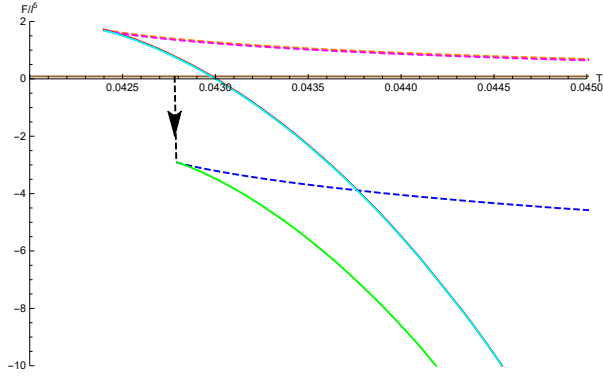
When solving eqn. (53) for \tilde{r}_+ in terms of \tilde{T} , the solution $\tilde{r}_+(\tilde{T})$ is often a multivalued function like what is shown in FIG. 1(b). The parameters \tilde{h} and \tilde{q} determine the number of the branches of $\tilde{r}_+(\tilde{T})$ and the phase structure of the black hole. In what follows, we find four regions in the \tilde{h} - \tilde{q} plane if we only consider the number of branches of $\tilde{r}_+(\tilde{T})$, taking into account for phase transition, Region I has five subregions. Each region has the distinct behavior of the branches and the phase structure:



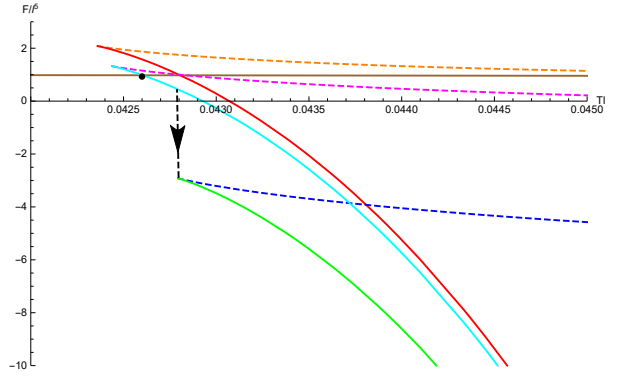
(a) Region I: $h/l^{1.5} = 1$ and $q/l^{4.5} = 0.02$.



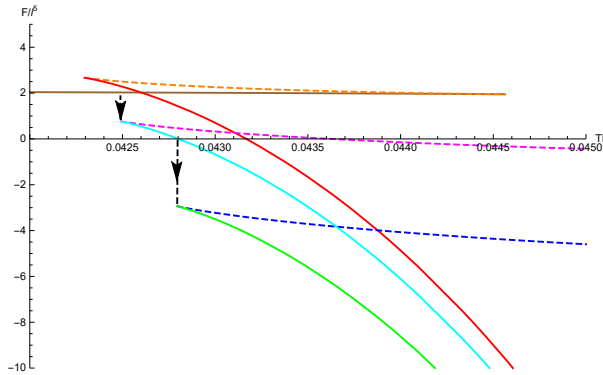
(b) Region I5: $h/l^{1.5} = 0.5$ and $q/l^{4.5} = 0.02$. There is a first order phase transition between Smallest BH and Large BH.



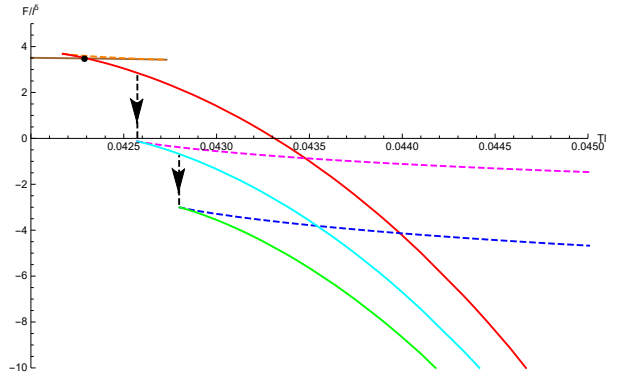
(c) Region I4: $h/l^{1.5} = 1$ and $q/l^{4.5} = 0.001$. There is a zeroth order phase transition between Smallest BH and Large BH.



(d) Region I3: $h/l^{1.5} = 1$ and $q/l^{4.5} = 0.02$. There is a first order phase transition between Smallest BH and Larger BH and a zeroth order phase transition between Larger BH and Large BH.



(e) Region I2: $h/l^{1.5} = 1$ and $q/l^{4.5} = 0.05$. There is a zeroth order phase transition between Smallest BH and Larger BH and a zeroth order phase transition between Larger BH and Large BH.

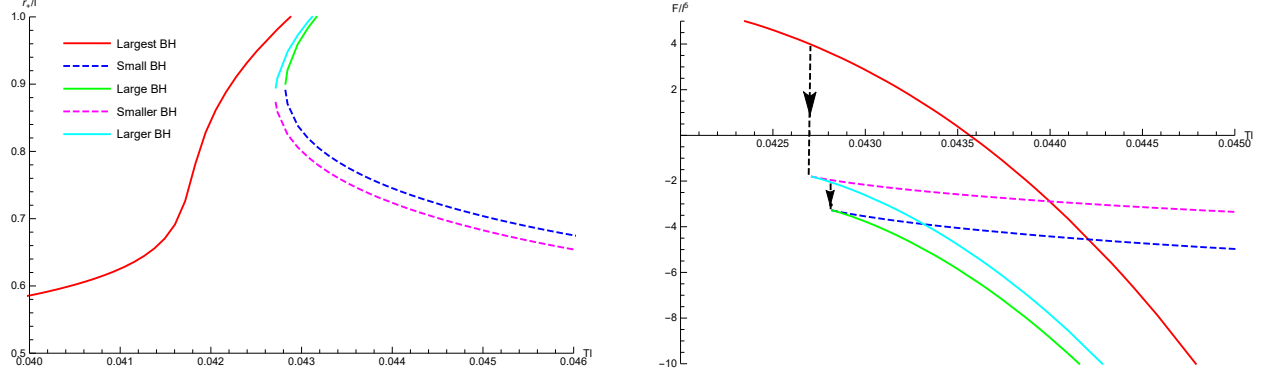


(f) Region I1: $h/l^{1.5} = 1$ and $q/l^{4.5} = 0.1$. There is a first order phase transition between Smallest BH and Largest BH, a zeroth order phase transition between Largest BH and Larger BH and a zeroth order phase transition between

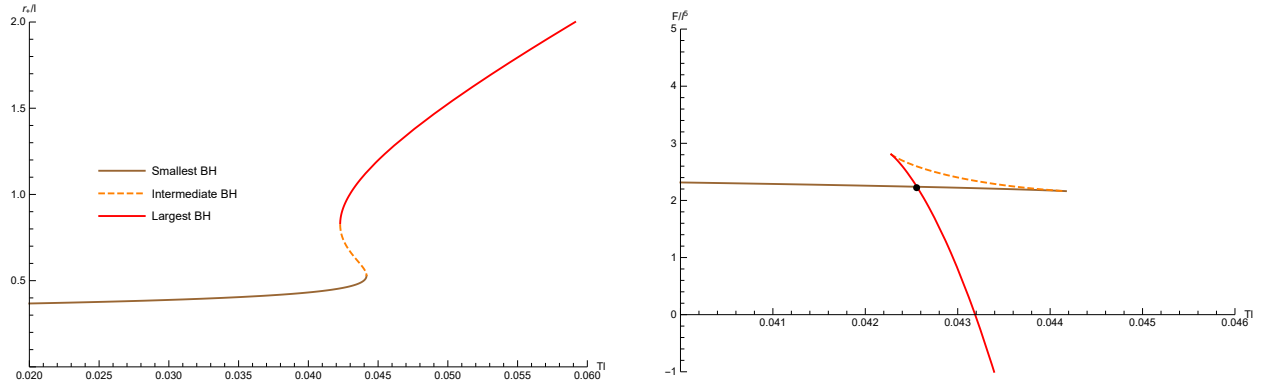
$\tilde{h} > 0, \tilde{q} > 0$	$\tilde{T}'(0)$	$\tilde{T}'(+\infty)$	Solution of $\tilde{T}''(\tilde{r}_+) = 0$	Extremums of $\tilde{T}'(\tilde{r}_+)$
$T_1, \tilde{h}^4 D_1(\tilde{h}, \tilde{q}) > -2 \left(\frac{15}{28}\right)^4$	∞	$\frac{7}{4\pi}$	$\tilde{r}_1 > 0$	$\tilde{T}'_{min}(\tilde{r}_1) < 0$
$T_1, \tilde{h}^4 D_1(\tilde{h}, \tilde{q}) < -2 \left(\frac{15}{28}\right)^4$	∞	$\frac{7}{4\pi}$	$\tilde{r}_1 > 0$	$\tilde{T}'_{min}(\tilde{r}_1) > 0$
$T_2, x < 1$	$-\infty$	$\frac{7}{4\pi}$	None, $\tilde{T}''(\tilde{r}_+) > 0$	None
$T_3, x < 1$	$-\infty$	$\frac{7}{4\pi}$	None, $\tilde{T}''(\tilde{r}_+) > 0$	None

TABLE I: Solution of $\tilde{T}'_i(\tilde{r}_+) = 0$ and the local extremums of $\tilde{T}'_i(\tilde{r}_+)$ in various cases.

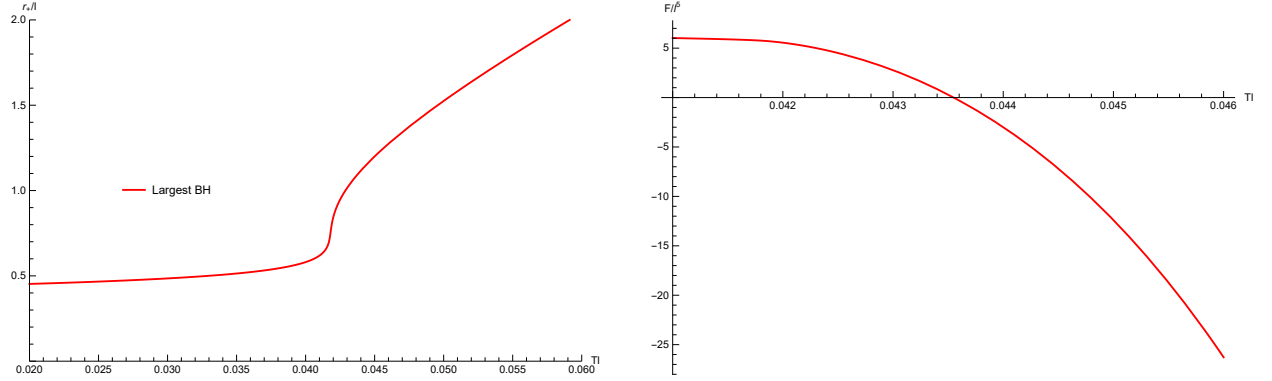
- Region I: $x < 1$ and $\tilde{T}'_1(\tilde{r}_1) < 0$, where \tilde{r}_1 is the solution of $\tilde{T}''_1(\tilde{r}_+) = 0$. In this region, $\tilde{T}'_1(\tilde{r}_+) = 0$ has two solutions $\tilde{r}_+ = \tilde{r}_{\max}$ and $\tilde{r}_+ = \tilde{r}_{\min}$ with $\tilde{r}_{\max} < \tilde{r}_1 < \tilde{r}_{\min}$. Since $\tilde{T}'_1(+\infty) = +\infty$, $\tilde{T}'_1(\tilde{r}_+)$ has a local maximum of $\tilde{T}'_{1\max} = \tilde{T}'_1(\tilde{r}_{\max})$ at $\tilde{r}_+ = \tilde{r}_{\max}$ and a local minimum of $\tilde{T}'_{1\min} = \tilde{T}'_1(\tilde{r}_{\min})$ at $\tilde{r}_+ = \tilde{r}_{\min}$. There are three branches for $\tilde{r}_{+1}(\tilde{T})$: smallest BH for $0 \leq \tilde{T}_1 \leq \tilde{T}'_{1\max}$, intermediate BH for $\tilde{T}'_{1\min} \leq \tilde{T}_1 \leq \tilde{T}'_{1\max}$ and largest BH for $\tilde{T}_1 \geq \tilde{T}'_{1\min}$, there are two branches for $\tilde{r}_{+2}(\tilde{T})$: small BH for $0 \leq \tilde{T}_2 \leq \tilde{T}'_{2\min}$ and large BH for $\tilde{T}_2 \geq \tilde{T}'_{2\min}$, and there are also two branches for $\tilde{r}_{+3}(\tilde{T})$: smaller BH for $0 \leq \tilde{T}_3 \leq \tilde{T}'_{3\min}$ and larger BH for $\tilde{T}_3 \geq \tilde{T}'_{3\min}$. The dependence of \tilde{r}_+ to T is displayed in the left panel of FIG. 3(a). The Gibbs free energy of the three branches is plotted in the follow five panels for different subregions. The smallest BH, large BH, larger BH and largest BH branches are thermally stable. (When $x = 1$, there are three subregions, and they are similar with the case I5, I2, I1 respectively, except \tilde{T}_2 and \tilde{T}'_2 merge into one.)
- Region II: $x < 1$ and $\tilde{T}'_1(\tilde{r}_1) \geq 0$. In this region, $\tilde{T}'_1(\tilde{r}_+) \geq \tilde{T}'_1(\tilde{r}_1) \geq 0$ and hence $\tilde{T}'_1(\tilde{r}_+)$ is an increasing function. So there is only one branch for $\tilde{r}_{+1}(\tilde{T})$: largest BH, which is thermally stable, there are two branches for $\tilde{r}_{+2}(\tilde{T})$: small BH for $0 \leq \tilde{T}_2 \leq \tilde{T}'_{2\min}$ and large BH for $\tilde{T}_2 \geq \tilde{T}'_{2\min}$, and there are two branches for $\tilde{r}_{+3}(\tilde{T})$: smaller BH for $0 \leq \tilde{T}_3 \leq \tilde{T}'_{3\min}$ and larger BH for $\tilde{T}_3 \geq \tilde{T}'_{3\min}$, and these are displayed in the left panel of FIG. 4(a). The Gibbs free energy of the three branches is plotted in the right panel. The large BH, larger BH and largest BH branches are thermally stable. (If $x = 1$, it is similar except \tilde{T}_2 and \tilde{T}'_3 merge into one.)
- Region III: $x > 1$ and $\tilde{T}'_1(\tilde{r}_1) < 0$. In this region, $\tilde{T}'_1(\tilde{r}_+) = 0$ has two solutions $\tilde{r}_+ = \tilde{r}_{\max}$ and \tilde{r}_{\min} with $\tilde{r}_{\max} < \tilde{r}_1 < \tilde{r}_{\min}$. Since $\tilde{T}'_1(+\infty) = +\infty$, $\tilde{T}'_1(\tilde{r}_+)$ has a local



(a) Region II: $h/l^{1.5} = 1$ and $q/l^{4.5} = 0.2$. There is a zeroth order phase transition between Largest BH and Larger BH and a zeroth order phase transition between Larger BH and Large BH.



(b) Region III: $h/l^{1.5} = 0.5$ and $q/l^{4.5} = 0.1$. There is a first order phase transition between Smallest BH and Largest BH.



(c) Region IV: $h/l^{1.5} = 0.5$ and $q/l^{4.5} = 0.3$. There is no phase transition.

FIG. 4: Plot of \tilde{r}_+ , \tilde{F} against \tilde{T} for PL-AdS black holes in Regions II, III and IV. The number of branches is different in these regions. The intermediate BH, small BH and smaller are always thermally unstable, others are always thermally stable.

maximum of $\tilde{T}_{1\max} = \tilde{T}_1(\tilde{r}_{\max})$ at $\tilde{r}_+ = \tilde{r}_{\max}$ and a local minimum of $\tilde{T}_{1\min} = \tilde{T}_1(\tilde{r}_{\min})$ at $\tilde{r}_+ = \tilde{r}_{\min}$. There are three branches for $\tilde{r}_{+1}(\tilde{T})$: smallest BH for $0 \leq \tilde{T}_1 \leq \tilde{T}_{1\max}$, intermediate BH for $\tilde{T}_{1\min} \leq \tilde{T}_1 \leq \tilde{T}_{1\max}$ and largest BH for $\tilde{T}_1 \geq \tilde{T}_{1\min}$. $\tilde{r}_{+2}(\tilde{T})$ and $\tilde{r}_{+3}(\tilde{T})$ don't exist, so there is a first order phase transition. These are displayed in the left panel of FIG. 4(b). The Gibbs free energy of the three branches is plotted in the right panel. The smallest BH and largest BH branches are thermally stable.

- Region IV: $x > 1$ and $\tilde{T}'_1(\tilde{r}_1) \geq 0$. In this region, $\tilde{T}'_1(\tilde{r}_+) \geq \tilde{T}'_1(\tilde{r}_1) \geq 0$ and hence $\tilde{T}_1(\tilde{r}_+)$ is an increasing function. So there is only one branch for $\tilde{r}_{+1}(\tilde{T})$: largest BH, which is thermally stable, $\tilde{r}_{+2}(\tilde{T})$ and $\tilde{r}_{+3}(\tilde{T})$ don't exist, so there is no phase transition in this region. These are displayed in the left panel of FIG. 4(c). The Gibbs free energy is plotted in the right panel.

We have marked first order phase transition with black point and zeroth order phase transition with arrow. In FIG. 5, we plot these eight regions in the \tilde{h} - \tilde{q} plane.

We can now discuss the critical behavior and phase structure of black holes in two cases. The critical line is the boundary between the region in which $\tilde{T}(\tilde{r}_+)$ has n extremums and that in which $\tilde{T}(\tilde{r}_+)$ has $n + 2$ extremums, determined by

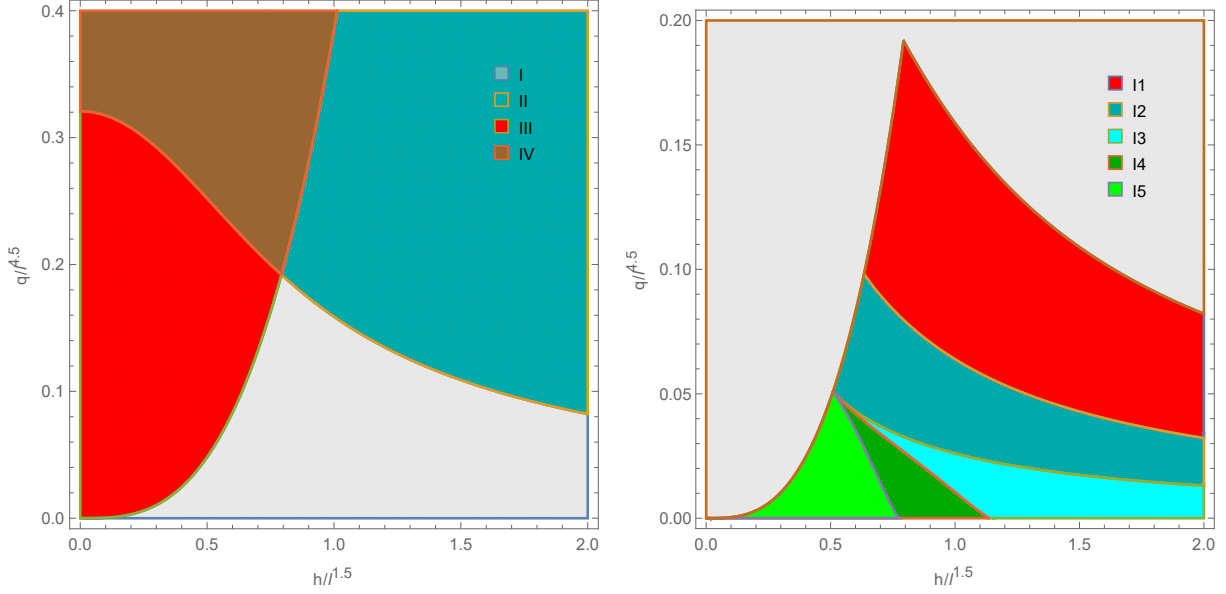
$$\frac{\partial \tilde{T}(\tilde{r}_+, \tilde{Q}, \tilde{a})}{\partial \tilde{r}_+} = 0 \text{ and } \frac{\partial^2 \tilde{T}(\tilde{r}_+, \tilde{Q}, \tilde{a})}{\partial \tilde{r}_+^2} = 0. \quad (61)$$

In the first case, q and h are fixed parameters, and the AdS radius l (the pressure P) varies. With fixed values of q and h , varying l would generate a curve in the \tilde{h} - \tilde{q} plane, which is determined by

$$\tilde{q}_l(\tilde{h}) = \frac{q}{h^3} \tilde{h}^3. \quad (62)$$

In FIG. 6, we plot $\tilde{q}_l(\tilde{h})$ for various values of q/h^3 . It shows that, there is always critical point for black holes. For $q/h^3 > 2\sqrt{3}/9$, as one starts from $P = 0$, $\tilde{q}_l(\tilde{h})$ always crosses the critical line and enters Region IV, in which there is no phase transition, from Region III, in which there is a first phase transition between smallest BH and largest BH. For $q/h^3 < 2\sqrt{3}/9$, as one starts from $P = 0$, $\tilde{q}_l(\tilde{h})$ always passes through five subregions, then crosses the critical line and enters Region II, in which there are two zeroth phase transitions, from largest BH to larger BH and from larger BH to large BH.

In the second case, h and P (l) are fixed parameters, and one varies \tilde{q} . As one increases \tilde{q} from $\tilde{q} = 0$, the black hole would experience different regions. And there is always a critical



(a) The four main regions in the \tilde{h} - \tilde{q} plane, each of which possesses the distinct behavior of the branches and the phase structure.

(b) The five subregions of Region I in the \tilde{h} - \tilde{q} plane, each of which possesses the distinct phase structure.

FIG. 5: The eight regions in the \tilde{h} - \tilde{q} plane for dyonic PMI AdS black holes. The color represents for the branch which it enters at first phase transition with increasing \tilde{T} from 0 (except Region IV), the darker color represents for zeroth order phase transition, the lighter color represents for first order phase transition.

point for any \tilde{h} since the critical line only has one end point at $\tilde{h} = 0$. In FIG 7, I plot that in the case of $\tilde{h} = 0.5$, $\tilde{h} = 0.6$, $\tilde{h} = 0.7$ and $\tilde{h} = 1$.

For $\tilde{h} \leq \tilde{h}_1 \simeq 0.51$, as one increases \tilde{q} from $\tilde{q} = 0$, the black hole would experience three regions, in which there occur the smallest BH/large BH first order phase transition \rightarrow the smallest BH/largest BH first order phase transition \rightarrow no phase transition, showed in FIG. 7(a).

For $\tilde{h} \geq \tilde{h}_1$, there is another region to across between the two regions mentioned above, in which there occurs the smallest BH/large BH zeroth order phase transition \rightarrow a smallest BH/larger BH first order phase transition and a larger BH/large BH zeroth phase transition \rightarrow a smallest BH/larger BH zeroth order phase transition and a larger BH/large BH zeroth phase transition. These are showed in FIG. 7(b).

When $\tilde{h} \geq \tilde{h}_2 \simeq 0.63$, the range of region that has a smallest BH/largest BH first order phase transition will expand to the left, which is showed in FIG. 7(c).

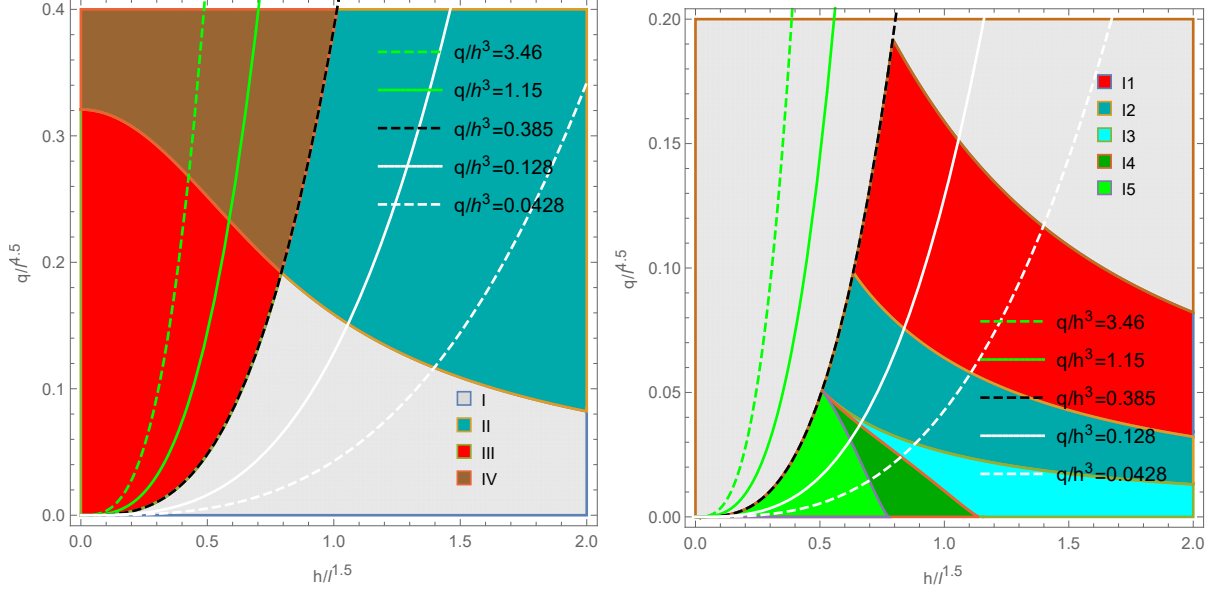


FIG. 6: In the case of varying P with fixed q and h , the system moves along $\tilde{q}_l(\tilde{h})$, which is displayed for various values of q/h^3 . There is always a critical point and the corresponding largest BH/smallest BH first order phase transition.

When $\tilde{h} \geq \tilde{h}_3 \simeq 0.76$, the smallest BH/large BH first order phase transition at left disappears, showed in FIG. 7(a) and the smallest BH/large BH zeroth order phase transition disappears when $\tilde{h} \geq \tilde{h}_4 \simeq 1.14$, it is reminiscent of FIG. 7(d), just cutting the Red line before Blue line at left.

IV. DISCUSSION AND CONCLUSION

We have investigated the thermodynamic behavior of d -dimensional dyonic PM AdS black holes in an extended phase space, which includes the conjugate pressure/volume quantities. It showed that the black hole's temperature T , charge q , horizon radius r_+ (thermodynamic volume V), the AdS radius l (pressure P) and the magnetic parameter h could be connected by

$$Tl = \tilde{T}(r_+/l, q/l^a, h/l^b), \quad (63)$$

where a and b depend on the dimension d and the power exponent p . In the canonical ensemble with fixed T and q , we found that the critical behavior and phase structure of the black hole are determined by $\tilde{q} \equiv q/l^a$ and $\tilde{h} \equiv h/l^b$.

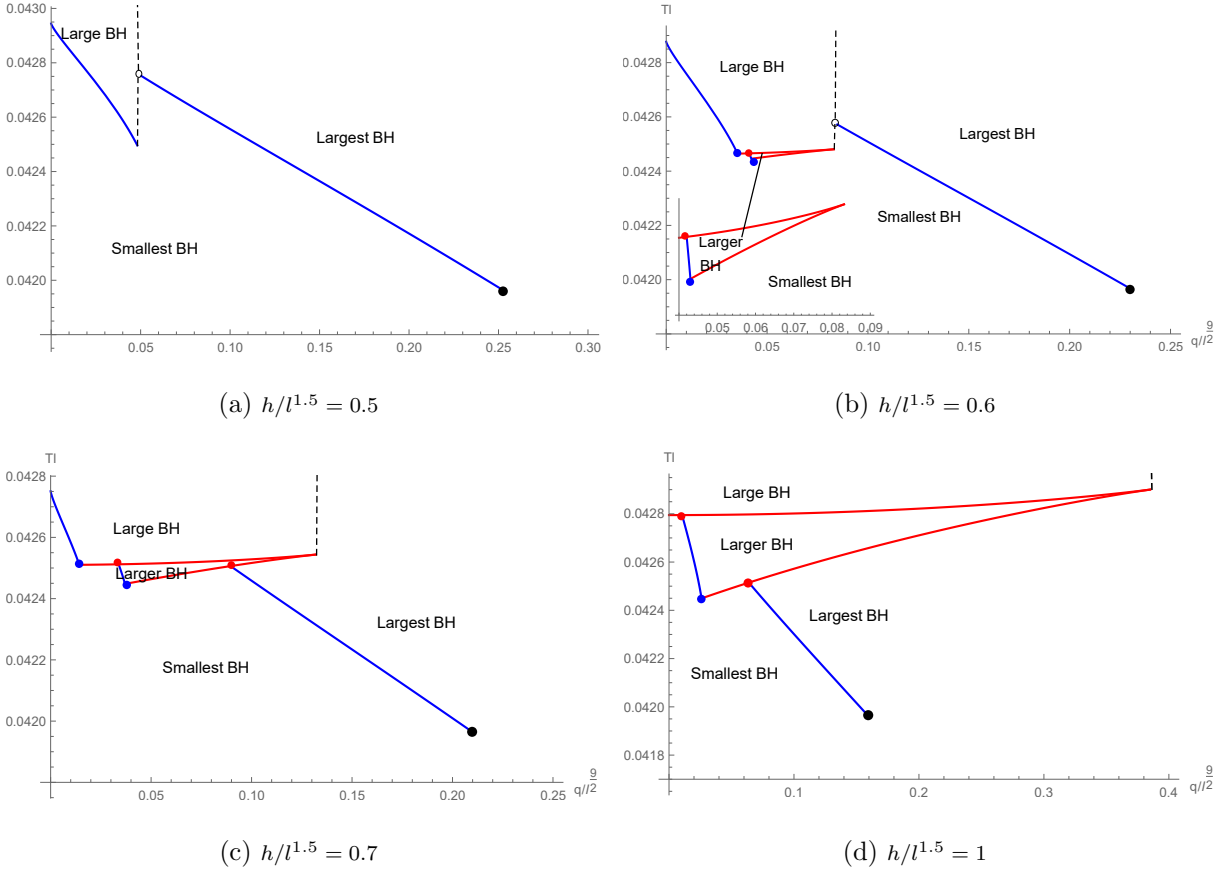


FIG. 7: The phase diagram in the \tilde{q} - \tilde{T} plane for PMI-AdS black holes with $h/l^{1.5} = 0.5$, $h/l^{1.5} = 0.6$, $h/l^{1.5} = 0.7$ and $h/l^{1.5} = 1$. The Blue line(point) represent for first order phase transition and the Red line (point) represent for zeroth order transition. The Black point represent for the critical point.

For 8-dimensional PM dyonic AdS black holes with an power exponent of 2, we examined their critical behavior and phase structure, whose dependence on \tilde{q} and \tilde{h} was plotted in FIG. 5. There are 8 regions in FIG. 5, and each region has a different phase behavior. Unlike other black holes, the temperature $\tilde{T}(r_+/l, q/l^{4.5}, h/l^{1.5})$ of PM dyonic AdS black holes could be more than one when some parameter configurations of $q/l^{4.5}$ and $h/l^{1.5}$ vary. If we discuss them separately, one of them (\tilde{T}_1 in this case) likes the case of RN-AdS black holes and the other two (if exist) like the case of Schwarzschild-AdS black holes. The combination of them results in these rich phase structures and phase behaviors.

The thermodynamically preferred phases, along with the zeroth and first order phase transitions and critical points, were displayed in FIG. 7 for the black holes. We examined thermal stabilities of the black holes and found that all the thermodynamically preferred

phases are thermally stable.

V. ACKNOWLEDGEMENT

We are grateful to thank Peng Wang and Yuchen Huang for useful discussions. This work is supported by NSFC (Grant No.11947408).

-
- [1] Werner Israel. Event horizons in static vacuum space-times. *Phys. Rev.*, 164:1776–1779, 1967. [doi:10.1103/PhysRev.164.1776](https://doi.org/10.1103/PhysRev.164.1776).
 - [2] S.W. Hawking. Gravitational radiation from colliding black holes. *Phys. Rev. Lett.*, 26:1344–1346, 1971. [doi:10.1103/PhysRevLett.26.1344](https://doi.org/10.1103/PhysRevLett.26.1344).
 - [3] Jacob D Bekenstein. Black holes and the second law. *Lett. Nuovo Cim.*, 4(15):737–740, 1972. [doi:10.1007/BF02757029](https://doi.org/10.1007/BF02757029).
 - [4] Jacob D. Bekenstein. Black holes and entropy. *Phys. Rev. D*, 7:2333–2346, Apr 1973. URL: <https://link.aps.org/doi/10.1103/PhysRevD.7.2333>, [doi:10.1103/PhysRevD.7.2333](https://doi.org/10.1103/PhysRevD.7.2333).
 - [5] James M. Bardeen, B. Carter, and S.W. Hawking. The Four laws of black hole mechanics. *Commun. Math. Phys.*, 31:161–170, 1973. [doi:10.1007/BF01645742](https://doi.org/10.1007/BF01645742).
 - [6] S.W. Hawking. Particle Creation by Black Holes. In *1st Oxford Conference on Quantum Gravity*, pages 219–267, 8 1975.
 - [7] S.W. Hawking and Don N. Page. Thermodynamics of Black Holes in anti-De Sitter Space. *Commun. Math. Phys.*, 87:577, 1983. [doi:10.1007/BF01208266](https://doi.org/10.1007/BF01208266).
 - [8] G.W. Gibbons and S.W. Hawking. Cosmological Event Horizons, Thermodynamics, and Particle Creation. *Phys. Rev. D*, 15:2738–2751, 1977. [doi:10.1103/PhysRevD.15.2738](https://doi.org/10.1103/PhysRevD.15.2738).
 - [9] Juan Martin Maldacena. The Large N limit of superconformal field theories and supergravity. *Int. J. Theor. Phys.*, 38:1113–1133, 1999. [arXiv:hep-th/9711200](https://arxiv.org/abs/hep-th/9711200), [doi:10.1023/A:1026654312961](https://doi.org/10.1023/A:1026654312961).
 - [10] Edward Witten. Anti-de Sitter space, thermal phase transition, and confinement in gauge theories. *Adv. Theor. Math. Phys.*, 2:505–532, 1998. [arXiv:hep-th/9803131](https://arxiv.org/abs/hep-th/9803131), [doi:10.4310/ATMP.1998.v2.n3.a3](https://doi.org/10.4310/ATMP.1998.v2.n3.a3).
 - [11] Andrew Chamblin, Roberto Emparan, Clifford V. Johnson, and Robert C. Myers. Charged

- AdS black holes and catastrophic holography. *Phys. Rev. D*, 60:064018, Aug 1999. URL: <https://link.aps.org/doi/10.1103/PhysRevD.60.064018>, [arXiv:hep-th/9902170](https://arxiv.org/abs/hep-th/9902170), [doi:10.1103/PhysRevD.60.064018](https://doi.org/10.1103/PhysRevD.60.064018).
- [12] Andrew Chamblin, Roberto Emparan, Clifford V. Johnson, and Robert C. Myers. Holography, thermodynamics and fluctuations of charged AdS black holes. *Phys. Rev. D*, 60:104026, Oct 1999. URL: <https://link.aps.org/doi/10.1103/PhysRevD.60.104026>, [arXiv:hep-th/9904197](https://arxiv.org/abs/hep-th/9904197), [doi:10.1103/PhysRevD.60.104026](https://doi.org/10.1103/PhysRevD.60.104026).
- [13] Brian P. Dolan. Pressure and volume in the first law of black hole thermodynamics. *Class. Quant. Grav.*, 28:235017, 2011. [arXiv:1106.6260](https://arxiv.org/abs/1106.6260), [doi:10.1088/0264-9381/28/23/235017](https://doi.org/10.1088/0264-9381/28/23/235017).
- [14] David Kubiznak and Robert B. Mann. P-V criticality of charged AdS black holes. *JHEP*, 07:033, 2012. [arXiv:1205.0559](https://arxiv.org/abs/1205.0559), [doi:10.1007/JHEP07\(2012\)033](https://doi.org/10.1007/JHEP07(2012)033).
- [15] David Kastor, Sourya Ray, and Jennie Traschen. Enthalpy and the Mechanics of AdS Black Holes. *Class. Quant. Grav.*, 26:195011, 2009. [arXiv:0904.2765](https://arxiv.org/abs/0904.2765), [doi:10.1088/0264-9381/26/19/195011](https://doi.org/10.1088/0264-9381/26/19/195011).
- [16] Shao-Wen Wei and Yu-Xiao Liu. Critical phenomena and thermodynamic geometry of charged Gauss-Bonnet AdS black holes. *Phys. Rev. D*, 87(4):044014, Feb 2013. URL: <https://link.aps.org/doi/10.1103/PhysRevD.87.044014>, [arXiv:1209.1707](https://arxiv.org/abs/1209.1707), [doi:10.1103/PhysRevD.87.044014](https://doi.org/10.1103/PhysRevD.87.044014).
- [17] Rong-Gen Cai, Li-Ming Cao, Li Li, and Run-Qiu Yang. P-V criticality in the extended phase space of Gauss-Bonnet black holes in AdS space. *JHEP*, 09:005, 2013. [arXiv:1306.6233](https://arxiv.org/abs/1306.6233), [doi:10.1007/JHEP09\(2013\)005](https://doi.org/10.1007/JHEP09(2013)005).
- [18] Wei Xu and Liu Zhao. Critical phenomena of static charged AdS black holes in conformal gravity. *Phys. Lett. B*, 736:214–220, 2014. [arXiv:1405.7665](https://arxiv.org/abs/1405.7665), [doi:10.1016/j.physletb.2014.07.019](https://doi.org/10.1016/j.physletb.2014.07.019).
- [19] Antonia M. Frassino, David Kubiznak, Robert B. Mann, and Fil Simovic. Multiple Reentrant Phase Transitions and Triple Points in Lovelock Thermodynamics. *JHEP*, 09:080, 2014. [arXiv:1406.7015](https://arxiv.org/abs/1406.7015), [doi:10.1007/JHEP09\(2014\)080](https://doi.org/10.1007/JHEP09(2014)080).
- [20] M. H. Dehghani, S. Kamrani, and A. Sheykhi. $P-V$ criticality of charged dilatonic black holes. *Phys. Rev. D*, 90(10):104020, 2014. [arXiv:1505.02386](https://arxiv.org/abs/1505.02386), [doi:10.1103/PhysRevD.90.104020](https://doi.org/10.1103/PhysRevD.90.104020).
- [21] Robie A. Hennigar, Wilson G. Brenna, and Robert B. Mann. $P-v$ criticality in quasitopological gravity. *JHEP*, 07:077, 2015. [arXiv:1505.05517](https://arxiv.org/abs/1505.05517), [doi:10.1007/JHEP07\(2015\)077](https://doi.org/10.1007/JHEP07(2015)077).

- [22] Olivera Miskovic and Rodrigo Olea. Quantum Statistical Relation for black holes in nonlinear electrodynamics coupled to Einstein-Gauss-Bonnet AdS gravity. *Phys. Rev. D*, 83:064017, 2011. [arXiv:1012.4867](#), [doi:10.1103/PhysRevD.83.064017](#).
- [23] Olivera Miskovic and Rodrigo Olea. Conserved charges for black holes in Einstein-Gauss-Bonnet gravity coupled to nonlinear electrodynamics in AdS space. *Phys. Rev. D*, 83:024011, 2011. [arXiv:1009.5763](#), [doi:10.1103/PhysRevD.83.024011](#).
- [24] Harald H. Soleng. Charged black points in general relativity coupled to the logarithmic U(1) gauge theory. *Phys. Rev. D*, 52:6178–6181, 1995. [arXiv:hep-th/9509033](#), [doi:10.1103/PhysRevD.52.6178](#).
- [25] Eloy Ayon-Beato and Alberto Garcia. Regular black hole in general relativity coupled to nonlinear electrodynamics. *Phys. Rev. Lett.*, 80:5056–5059, 1998. [arXiv:gr-qc/9911046](#), [doi:10.1103/PhysRevLett.80.5056](#).
- [26] Hideki Maeda, Mokhtar Hassaine, and Cristian Martinez. Lovelock black holes with a nonlinear Maxwell field. *Phys. Rev. D*, 79:044012, 2009. [arXiv:0812.2038](#), [doi:10.1103/PhysRevD.79.044012](#).
- [27] S.H. Hendi, B. Eslam Panah, S. Panahiyan, and A. Sheykhi. Dilatonic BTZ black holes with power-law field. *Phys. Lett. B*, 767:214–225, 2017. [arXiv:1703.03403](#), [doi:10.1016/j.physletb.2017.01.066](#).
- [28] Jun Tao, Peng Wang, and Haitang Yang. Testing holographic conjectures of complexity with Born–Infeld black holes. *Eur. Phys. J. C*, 77(12):817, 2017. [arXiv:1703.06297](#), [doi:10.1140/epjc/s10052-017-5395-3](#).
- [29] Xiaobo Guo, Peng Wang, and Haitang Yang. Membrane Paradigm and Holographic DC Conductivity for Nonlinear Electrodynamics. *Phys. Rev. D*, 98(2):026021, 2018. [arXiv:1711.03298](#), [doi:10.1103/PhysRevD.98.026021](#).
- [30] Benrong Mu, Peng Wang, and Haitang Yang. Holographic DC Conductivity for a Power-law Maxwell Field. *Eur. Phys. J. C*, 78(12):1005, 2018. [arXiv:1711.06569](#), [doi:10.1140/epjc/s10052-018-6491-8](#).
- [31] Peng Wang, Houwen Wu, and Haitang Yang. Holographic DC Conductivity for Backreacted Nonlinear Electrodynamics with Momentum Dissipation. *Eur. Phys. J. C*, 79(1):6, 2019. [arXiv:1805.07913](#), [doi:10.1140/epjc/s10052-018-6503-8](#).
- [32] Peng Wang, Houwen Wu, and Haitang Yang. Thermodynamics and Phase Transitions of

- Nonlinear Electrodynamics Black Holes in an Extended Phase Space. *JCAP*, 04(04):052, 2019. [arXiv:1808.04506](#), [doi:10.1088/1475-7516/2019/04/052](#).
- [33] Tianhao Bai, Wei Hong, Benrong Mu, and Jun Tao. Weak cosmic censorship conjecture in the nonlinear electrodynamics black hole under the charged scalar field. *Commun. Theor. Phys.*, 72(1):015401, 2020. [doi:10.1088/1572-9494/ab544b](#).
- [34] Peng Wang, Houwen Wu, and Haitang Yang. Thermodynamics and Weak Cosmic Censorship Conjecture in Nonlinear Electrodynamics Black Holes via Charged Particle Absorption. 4 2019. [arXiv:1904.12365](#).
- [35] Qingyu Gan, Peng Wang, and Haitang Yang. Temperature Dependence of In-plane Resistivity and Inverse Hall Angle in NLED Holographic Model. *Commun. Theor. Phys.*, 71(5):577, 2019. [arXiv:1808.06158](#), [doi:10.1088/0253-6102/71/5/577](#).
- [36] Peng Wang, Houwen Wu, and Haitang Yang. Thermodynamics and Phase Transition of a Nonlinear Electrodynamics Black Hole in a Cavity. *JHEP*, 07:002, 2019. [arXiv:1901.06216](#), [doi:10.1007/JHEP07\(2019\)002](#).
- [37] Sharmanthie Fernando and Don Krug. Charged black hole solutions in Einstein-Born-Infeld gravity with a cosmological constant. *Gen. Rel. Grav.*, 35:129–137, 2003. [arXiv:hep-th/0306120](#), [doi:10.1023/A:1021315214180](#).
- [38] De-Cheng Zou, Shao-Jun Zhang, and Bin Wang. Critical behavior of Born-Infeld AdS black holes in the extended phase space thermodynamics. *Phys. Rev. D*, 89(4):044002, 2014. [arXiv:1311.7299](#), [doi:10.1103/PhysRevD.89.044002](#).
- [39] S.H. Hendi and M.H. Vahidinia. Extended phase space thermodynamics and P-V criticality of black holes with a nonlinear source. *Phys. Rev. D*, 88(8):084045, 2013. [arXiv:1212.6128](#), [doi:10.1103/PhysRevD.88.084045](#).
- [40] Jie-Xiong Mo, Gu-Qiang Li, and Xiao-Bao Xu. Effects of power-law Maxwell field on the critical phenomena of higher dimensional dilaton black holes. *Phys. Rev. D*, 93(8):084041, 2016. [arXiv:1601.05500](#), [doi:10.1103/PhysRevD.93.084041](#).
- [41] Pavan Kumar Yerra and Bhamidipati Chandrasekhar. Heat engines at criticality for nonlinearly charged black holes. *Mod. Phys. Lett. A*, 34(27):1950216, 2019. [arXiv:1806.08226](#), [doi:10.1142/S021773231950216X](#).
- [42] Cao H. Nam. Non-linear charged dS black hole and its thermodynamics and phase transitions. *Eur. Phys. J. C*, 78(5):418, 2018. [doi:10.1140/epjc/s10052-018-5922-x](#).

- [43] Mokhtar Hassaine and Cristian Martinez. Higher-dimensional black holes with a conformally invariant Maxwell source. *Phys. Rev. D*, 75:027502, 2007. [arXiv:hep-th/0701058](#), [doi:10.1103/PhysRevD.75.027502](#).
- [44] S.H. Hendi and H.R. Rastegar-Sedehi. Ricci flat rotating black branes with a conformally invariant Maxwell source. *Gen. Rel. Grav.*, 41:1355–1366, 2009. [arXiv:1007.2475](#), [doi:10.1007/s10714-008-0711-8](#).
- [45] S.H. Hendi. Topological black holes in Gauss-Bonnet gravity with conformally invariant Maxwell source. *Phys. Lett. B*, 677:123–132, 2009. [arXiv:1007.2479](#), [doi:10.1016/j.physletb.2009.03.085](#).
- [46] Mokhtar Hassaine and Cristian Martinez. Higher-dimensional charged black holes solutions with a nonlinear electrodynamics source. *Class. Quant. Grav.*, 25:195023, 2008. [arXiv:0803.2946](#), [doi:10.1088/0264-9381/25/19/195023](#).
- [47] S.H. Hendi and B.Eslam Panah. Thermodynamics of rotating black branes in Gauss-Bonnet-nonlinear Maxwell gravity. *Phys. Lett. B*, 684:77–84, 2010. [arXiv:1008.0102](#), [doi:10.1016/j.physletb.2010.01.026](#).
- [48] S.H. Hendi. Slowly Rotating Black Holes in Einstein-Generalized Maxwell Gravity. *Prog. Theor. Phys.*, 124:493–502, 2010. [arXiv:1008.0544](#), [doi:10.1143/PTP.124.493](#).
- [49] S.H. Hendi. Rotating black branes in the presence of nonlinear electromagnetic field. *Eur. Phys. J. C*, 69:281–288, 2010. [arXiv:1008.0168](#), [doi:10.1140/epjc/s10052-010-1359-6](#).
- [50] S.H. Hendi. Rotating Black String with Nonlinear Source. *Phys. Rev. D*, 82:064040, 2010. [arXiv:1008.5210](#), [doi:10.1103/PhysRevD.82.064040](#).
- [51] Jiliang Jing, Qiyuan Pan, and Songbai Chen. Holographic Superconductors with Power-Maxwell field. *JHEP*, 11:045, 2011. [arXiv:1106.5181](#), [doi:10.1007/JHEP11\(2011\)045](#).
- [52] K.A. Bronnikov. Dyonic configurations in nonlinear electrodynamics coupled to general relativity. *Grav. Cosmol.*, 23(4):343–348, 2017. [arXiv:1708.08125](#), [doi:10.1134/S0202289317040053](#).
- [53] D.A. Rasheed. Nonlinear electrodynamics: Zeroth and first laws of black hole mechanics. 2 1997. [arXiv:hep-th/9702087](#).